This is a repository copy of *Pelagic seabirds reduce risk by flying into the eye of the storm*.

White Rose Research Online URL for this paper:
https://eprints.whiterose.ac.uk/191689/

Version: Supplemental Material

Article:

PNAS

Supporting Information for

Pelagic seabirds reduce risk by flying into the eye of the storm

Emmanouil Lempidakis[1*], Emily L. C. Shepard[1*], Andrew N. Ross[2], Sakiko Matsumoto[3], Shiho Koyama[3], Ichiro Takeuchi[4], Ken Yoda[3]

[1]Department of Biosciences, Swansea University, Swansea, United Kingdom.

[2]School of Earth and Environment, University of Leeds, Leeds, United Kingdom.

[3]Graduate School of Environmental Studies, Nagoya University, Furo-cho, Chikusa-ku, Nagoya 464-8601, Japan

[4]Department of Computer Science, Nagoya Institute of Technology, Nagoya 466-8555, Japan

*Emmanouil Lempidakis, Emily L. C. Shepard

Emails: e.m.lempidakis@gmail.com, e.l.c.shepard@swansea.ac.uk

This PDF file includes:

Supplementary text

Figures S1 to S5

Tables S1 to S4

Legends for Movies S1 to S7

SI References

Other supplementary materials for this manuscript include the following:

Movies S1 to S7

Supplementary Information Text

Estimation of flight directions relative to storm and land.

In order to identify whether birds were attracted to or avoided the storms, we estimated the flight direction with respect to the eye of the storm using equations 1 and 2:

$$FDS = FD - SA + 360 \qquad \{for\ FD < SA\} \qquad (1)$$

$$FDS = FD - SA \qquad \{for\ FD >= SA\} \qquad (2)$$

where FDS is the flight direction with respect to the eye $(0 - 360^{\circ})$ which was converted to the range of $0 - 180^{\circ}$, with 0° and 180° indicating flight straight towards and away respectively, FD is the GPS derived flight heading $(0 - 360^{\circ})$ and SA is the storm angle $(0 - 360^{\circ})$, which is the direction a bird would have to travel to fly straight to the eye of the storm.

To assess whether shearwaters show a distinct response depending on whether the storm is heading towards or away from the bird, we calculated the bird position with respect to the storm direction of travel using equations 3 and 4:

$$BP = SAP - SD + 360 \qquad \{for\ SAP < SD\} \qquad (3)$$

$$BP = SAP - SD \qquad \{for\ SAP >= SD\} \qquad (4)$$

where BP is the bird position with respect to the eye $(0 - 360^{\circ})$ which was converted to the range of $0 - 180^{\circ}$ with 0° indicating that the bird was located in-front of a storm and 180° exactly behind, SAP is the opposite direction from SA and SD is the direction to which a storm is travelling $(0 - 360^{\circ})$.

To assess whether shearwaters fly away from land to reduce the risk of being wrecked, we estimated the minimum distance to land in ArcMap 10.5.1 (ESRI, Redlands, California) and the flight direction with respect to the closest point on land at each bird location, using the equations 5 to 8:

$$FDL = |\, FD - LD\, | \qquad \{\text{for } LD \leq 180 \text{ and for } FD \leq 180\} \qquad (5)$$

$$FDL = FD + 360 - LD \qquad \{\text{for } LD > 180 \text{ and for } FD \leq 180\} \qquad (6)$$

$$FDL = LD + 360 - FD \qquad \{\text{for } LD \leq 180 \text{ and for } FD > 180\} \qquad (7)$$

$$FDL = |\, (360 - FD) - (360\text{-}LD)\, | \qquad \{\text{for } LD > 180 \text{ and for } FD > 180\} \qquad (8)$$

where FDL is the flight direction with respect to the closest location on land $(0 - 360°)$ which was converted to the range of $0 - 180°$, with $0°$ and $180°$ indicating flight straight towards land and away respectively and LD is the direction that a bird would have to fly to travel straight to that location $(0 - 360°)$.

Table S1. Tropical storms were categorized using the maximum wind speed within the Sea of Japan, provided by IBTrACS, and using the Japan Meteorological Agency (JMA) international classification. Maximum wind speed estimates within the Sea of Japan are given for both IBTrACS and ERA5, for the period that a storm travelled within the study area. We note that reanalyses tend to under-represent storms and especially the weaker tropical depressions/ storms, in terms of both intensity and spatial extent, with uncertainties increasing with decreasing strength (1).

Storm	Period	Max hourly wind speed (IBTrACS, m s^{-1})	Max hourly wind speed (ERA5, m s^{-1})	Classification (JMA)
Kompasu	02-03/09/2010	25.7	16.0	Severe tropical storm
Malou	07-08/09/2010	18.0	17.2	Tropical storm
Meranti	12/09/2010	14.9	21.6	Tropical depression
Fung-Wong	24-25/09/2014	15.9	13.4	Tropical depression
Goni	25-26/08/2015	33.4	24.4	Typhoon
Etau	09-11/09/2015	19.5	20.7	Tropical storm
Talim	17-18/09/2017	26.7	22.5	Severe tropical storm
Cimaron	23-24/08/2018	32.9	27.1	Typhoon
Soulik	24-25/08/2018	23.1	21.0	Tropical storm
Jebi	04/09/2018	41.1	24.5	Typhoon

Wind speed (m s⁻¹)

0 5 10 15 20 27

400 km
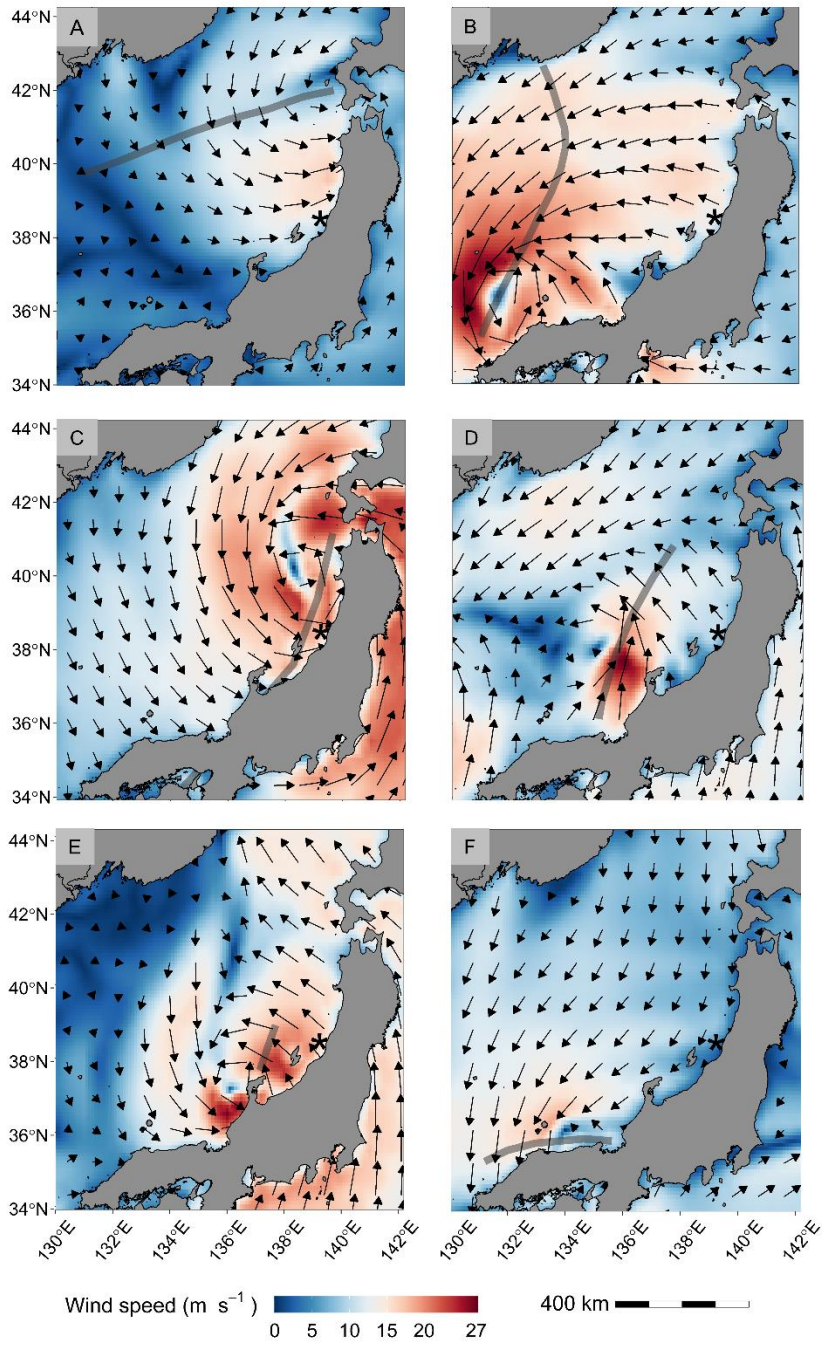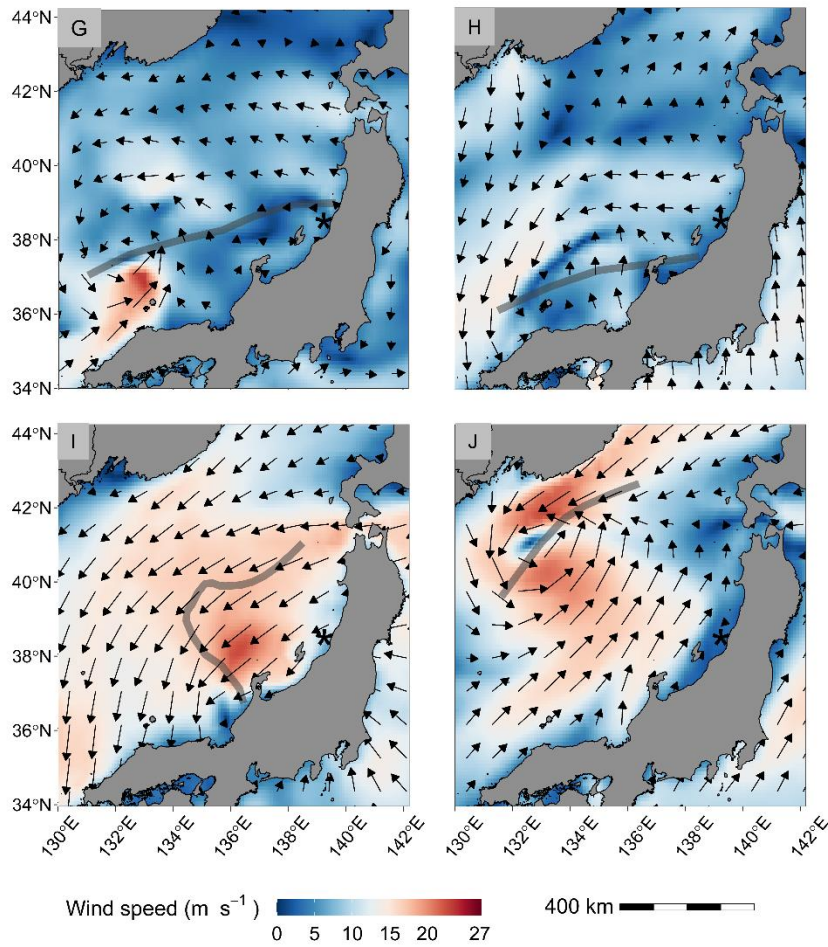
Figure S1. Wind speed and direction at the hour of the maximum estimated wind speed for each of the ten storms in the Sea of Japan. We note that wind speeds from ERA5 are subject to varying degrees of underestimation relative to IBTrACS data, and consequently we used the latter to classify storms (Table S1). The five strongest storms are given in panels A-E and the five weakest in panels F-J, in chronological order. (A) Kompasu, (B) Goni, (C) Talim, (D) Cimaron, (E) Jebi, (F) Malou, (G) Meranti, (H) Fung-Wong, (I) Etau , (J) Soulik. The path of each storm is indicated with a grey line.

Table S2. Generalized additive mixed effect models predicting flight direction relative to the storm track during the five strongest storms (model 1, n = 690) and during all ten storms (model 2, n = 1,556). From left to right: model terms indicating the base dimension (k) when this differed from the default value, effective degrees of freedom (edf) and p-values. Significance is indicated according to p-value: $p < 0.001$ (***), $p < 0.01$ (**), $p < 0.005$ (*).

	Term	Edf	P-value
Model 1: Flight	ti(Bird position, k=37)	16.0	< 0.001 ***
direction	ti(wind speed)	1.0	< 0.01 **
relative to five	ti(wind direction, wind speed)	7.5	< 0.001 ***
strongest storms	ti(Bird position, wind speed)	8.1	< 0.001 ***
	s(Storm ID)	2.5	< 0.001 ***
Model 2: Flight	ti(Bird position, k=37)	24.9	< 0.001 ***
direction	ti(wind speed)	1.0	< 0.001 ***
relative to ten	ti(wind direction, wind speed)	7.3	< 0.001 ***
storms	ti(Bird position, wind speed)	8.1	< 0.001 ***
	s(Storm ID)	7.8	< 0.001 ***
	AIC	**Adj. R^2**	**Dev. explained**
Model 1	7541	0.22	26.6 %
Model 2	16799	0.23	25.5 %

Five storms   **Ten storms**
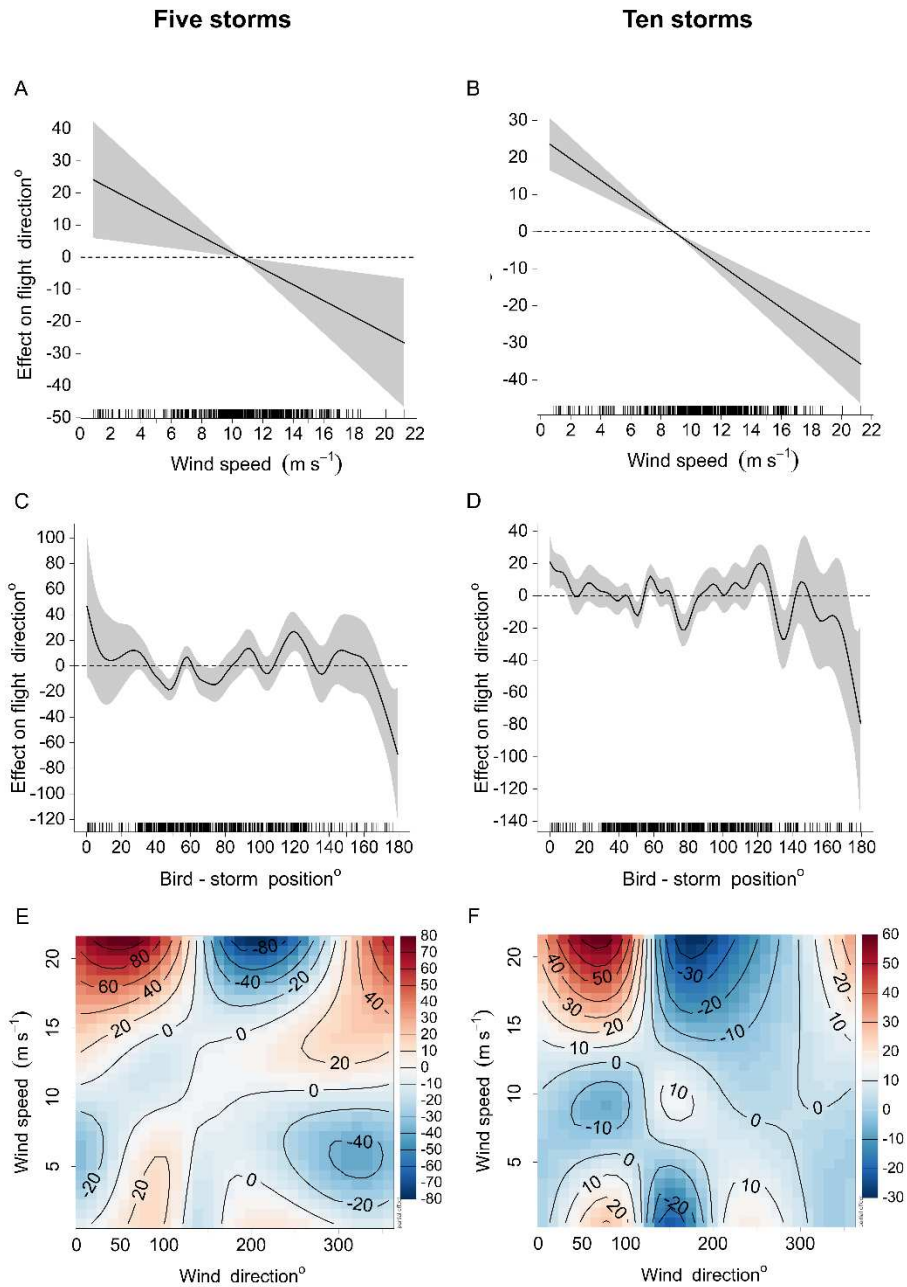
Figure S2. The partial effects of model parameters on bird flight direction in relation to

the storm eye. The responses to the five and ten strongest storms are given in the left and

right panels respectively. (A,B) show the response to wind speed, with birds flying

towards the eye in winds > 10 m s-1, (C,D) show the effect of bird position, where 0°

indicates birds were ahead of the storm's path and 180° indicates they were behind it, and

(E,F) give the interaction between wind speed and direction (the direction wind is coming from), showing that in strong northerly and easterly winds birds flew away from the storm (red), and in winds with a southerly component birds flew towards the eye of a storm (blue).

Table S3. Results of ten agent-based simulations operating in the five major storms. From left to right: storm name, mean wind speed at agent locations, percentage of agents flown, percentage and number of agents wrecked from the number of agents flown, percentage and number of agents flown with mean flight direction in relation to a storm ≤ 70o, percentage and number of agents reaching ≤ 30 and ≤ 60 km of the eye, from the agents capable of reaching the eye that were not wrecked. Overall, agents were attracted to storms that came within 60 – 170 km of the core foraging area but did not respond to storms that were further away.

Storm	Mean wind speed (m s-1)	Flown %	Wrecked % (agents)	Towards storm % (agents)	Reached ≤30 km % (agents)	Reached ≤ 60 km % (agents)
Kompasu	6.8	100	91.4 (3654)	0.1 (5)	17.5 (60)	55.21(158)
Goni	13.3	81.2	0.3 (9)	0 (0)	0.0 (0)	0 (0)
Talim	14.4	100	18.2 (727)	55.9 (2235)	33.9 (1093)	57.8 (1231)
Cimaron	11.5	100	3.3 (135)	39.7 (1586)	2.7 (62)	27.6 (866)
Jebi	15.1	100	1.2 (48)	61.9 (2475)	0.2 (1)	43.6 (397)

Table S4. Generalized additive mixed effect model predicting flight direction relative to the closest point on the mainland during all the ten storms studied (n = 1,562). From left to right: model terms indicating the base dimension (k) when this differed from the default value, effective degrees of freedom (edf) and p-values. Significance is indicated according to p-value: $p < 0.001$ (***), $p < 0.01$ (**), $p < 0.005$ (*).

	Term	Edf	P-value
Model 3: Flight	ti (bird-land distance)	2.3	< 0.001 ***
direction	ti(wind speed)	0.9	< 0.01 **
relative to land	ti(wind direction, wind speed)	7.4	< 0.001 ***
(ten storms)	ti(Bird position, wind speed)	0.0	n.s
	ti(bird-land distance , wind speed)	5.5	< 0.001 ***
	s(Storm ID)	7.8	< 0.001 ***
	AIC	**Adj. R^2**	**Dev. explained**
	16317	0.12	13.9 %
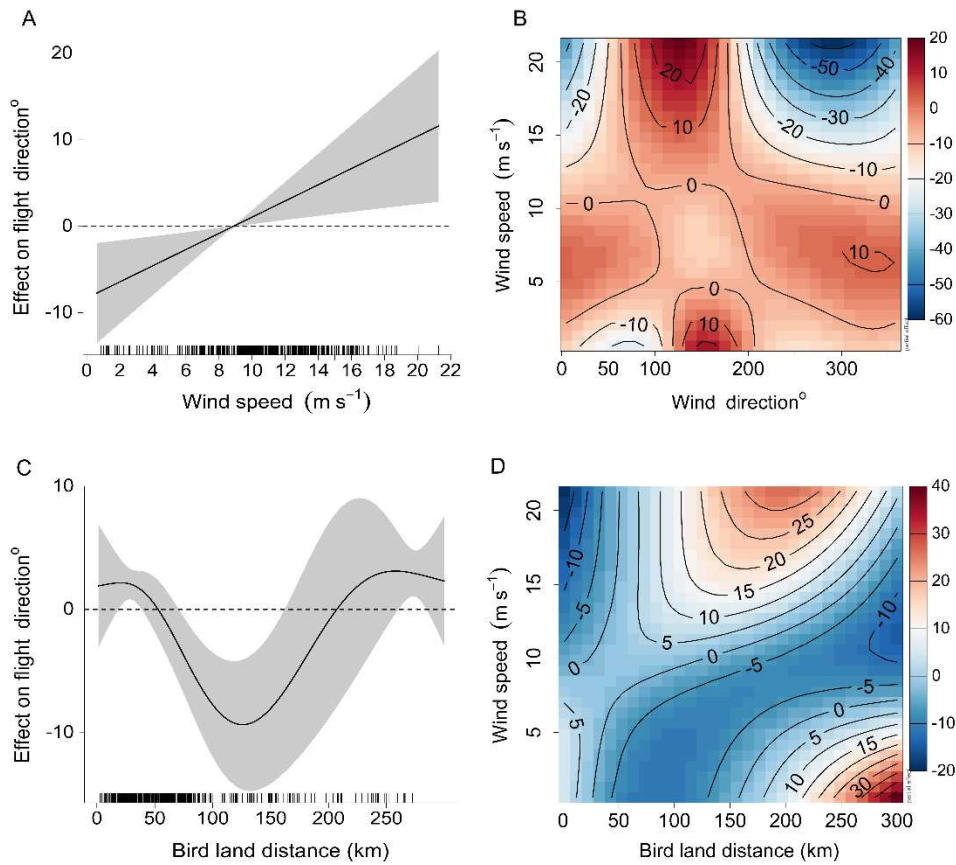
Figure S3. The partial effects of model parameters on flight direction with respect to land. (A) Birds flew away from land in strong winds (positive effect). (B) The interaction between wind speed and direction was also significant, with birds flying towards land (blue) in northerly and westerly winds, and away from land in easterly and southerly winds. (C) Distance to land also affected the tendency of birds to fly towards it, although the effect size was smaller, with birds flying away from land when they were < 50 km from it. This was complicated further by the interaction of wind speed and distance to land, (D), showing that while birds tended to fly away from land in strong winds, there were cases when birds were < 25 km from land and flew towards it. Inspection of the raw data showed that 3 birds were this distance to land in winds > 15 m s^{-1}. In each case the storm was 200-440 km away
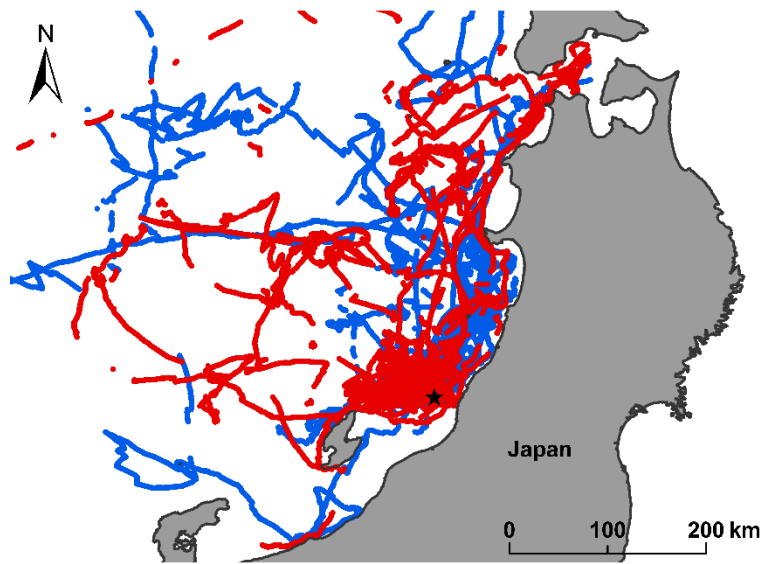
Figure S4. GPS locations in the Sea of Japan during the five strongest storms (red) and during all storms studied (blue). The colony on Awashima Island is indicated with a star.
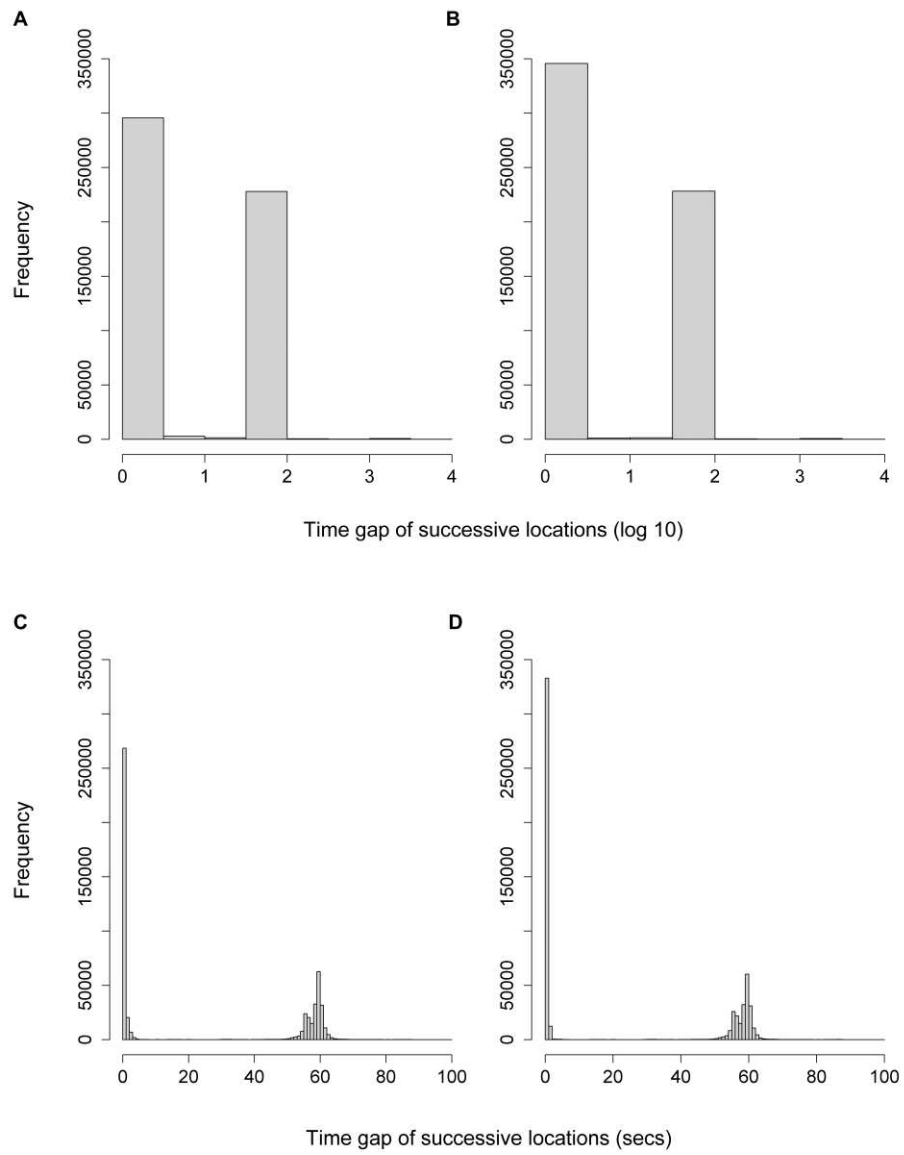
Figure S5. Frequency of time gaps between successive GPS locations in log 10 (A, B) and in seconds (C, D). Frequencies are given for the GPS dataset filtered by using a 25 m s^{-1} ground speed filter (A, C) and for the un-filtered dataset (B, D).

Movie S1 (separate file).

GPS tracks of streaked shearwaters during the passage of severe tropical storm Talim (black track) in 2017, animated over the wind field estimated by ERA5 reanalysis, wind speed ($m\ s^{-1}$).

Movie S2 (separate file).

GPS tracks of streaked shearwaters during the passage of typhoon Cimaron, tropical storm Soulik and typhoon Jebi (black tracks in order of appearance) in 2018, animated over the wind field estimated by ERA5 reanalysis, wind speed ($m\ s^{-1}$).

Movie S3 (separate file).

The tracks of 400 agents, programmed with the output of GAMM model 1, moving in the wind field in the Sea of Japan during the passage of severe tropical storm Kompasu (black track) in 2010.

Movie S4 (separate file).

The tracks of 400 agents, programmed with the output of GAMM model 1, moving in the wind field in the Sea of Japan during the passage of typhoon Goni (black track) in 2015.

Movie S5 (separate file).

The tracks of 400 agents, programmed with the output of GAMM model 1, moving in the wind field in the Sea of Japan during the passage of severe tropical storm Talim (black track) in 2017.

Movie S6 (separate file).

The tracks of 400 agents, programmed with the output of GAMM model 1, moving in the wind field in the Sea of Japan during the passage of typhoon Cimaron (black track) in 2018.

Movie S7 (separate file).

The tracks of 400 agents, programmed with the output of GAMM model 1, moving in the wind field in the Sea of Japan during the passage of typhoon Jebi (black track) in 2018.

SI References

1.   Hodges K, Cobb A, & Vidale PL (2017) How well are tropical cyclones represented in reanalysis datasets? *Journal of Climate* 30(14):5243-5264.